

Chemical composition of PM10 and PM1 at the high-altitude Himalayan station Nepal Climate Observatory-Pyramid (NCO-P) (5079 m a.s.l.)

S. Decesari, M. C. Facchini, C. Carbone, L. Giulianelli, M. Rinaldi, E. Finessi, S. Fuzzi, A. Marinoni, P. Cristofanelli, R. Duchi, et al.

▶ **To cite this version:**

S. Decesari, M. C. Facchini, C. Carbone, L. Giulianelli, M. Rinaldi, et al.. Chemical composition of PM10 and PM1 at the high-altitude Himalayan station Nepal Climate Observatory-Pyramid (NCO-P) (5079 m a.s.l.). Atmospheric Chemistry and Physics, 2010, 10 (10), pp.4583-4596. 10.5194/acp-10-4583-2010 . insu-00554278

HAL Id: insu-00554278

https://insu.hal.science/insu-00554278

Submitted on 27 Feb 2012

HAL is a multi-disciplinary open access archive for the deposit and dissemination of scientific research documents, whether they are published or not. The documents may come from teaching and research institutions in France or abroad, or from public or private research centers.

L'archive ouverte pluridisciplinaire **HAL**, est destinée au dépôt et à la diffusion de documents scientifiques de niveau recherche, publiés ou non, émanant des établissements d'enseignement et de recherche français ou étrangers, des laboratoires publics ou privés.

Atmos. Chem. Phys., 10, 4583–4596, 2010
www.atmos-chem-phys.net/10/4583/2010/
doi:10.5194/acp-10-4583-2010
© Author(s) 2010. CC Attribution 3.0 License.

Atmospheric Chemistry and Physics

Chemical composition of PM_{10} and PM_1 at the high-altitude Himalayan station Nepal Climate Observatory-Pyramid (NCO-P) (5079 m a.s.l.)

S. Decesari[1], M. C. Facchini[1], C. Carbone[1], L. Giulianelli[1], M. Rinaldi[1], E. Finessi[1], S. Fuzzi[1], A. Marinoni[1], P. Cristofanelli[1], R. Duchi[1], P. Bonasoni[1], E. Vuillermoz[2], J. Cozic[3], J. L. Jaffrezo[3], and P. Laj[3]

[1]Institute for Atmospheric Sciences and Climate (ISAC), CNR, Bologna, Italy
[2]Ev-K2-CNR Committee, Bergamo, Italy
[3]Laboratoire de Glaciologie et Géophysique de l'Environnement (LGGE), CNRS/University of Grenoble, Grenoble, France

Received: 30 October 2009 – Published in Atmos. Chem. Phys. Discuss.: 26 November 2009
Revised: 29 March 2010 – Accepted: 20 April 2010 – Published: 18 May 2010

Abstract. We report chemical composition data for PM_{10} and PM_1 from the Nepal Climate Observatory-Pyramid (NCO-P), the world's highest aerosol observatory, located at 5079 m a.s.l. at the foothills of Mt. Everest. Despite its high altitude, the average PM_{10} mass apportioned by the chemical analyses is of the order of 6 µg m^{-3} (i.e., 10 µg/scm), with almost a half of this mass accounted for by organic matter, elemental carbon (EC) and inorganic ions, the rest being mineral dust. Organic matter, in particular, accounted for by 2.0 µg m^{-3} (i.e., 3.6 µg/scm) on a yearly basis, and it is by far the major PM_{10} component beside mineral oxides. Non-negligible concentrations of EC were also observed (0.36 µg/scm), confirming that light-absorbing aerosol produced from combustion sources can be efficiently transported up the altitudes of Himalayan glaciers. The concentrations of carbonaceous and ionic aerosols follow a common time trend with a maximum in the premonsoon season, a minimum during the monsoon and a slow recovery during the postmonsoon and dry seasons, which is the same phenomenology observed for other Nepalese Himalayan sites in previous studies. Such seasonal cycle can be explained by the seasonal variations of dry and moist convection and of wet scavenging processes characterizing the climate of north Indian subcontinent. We document the effect of orographic transport of carbonaceous and sulphate particles upslope the Himalayas, showing that the valley breeze circulation, which is almost permanently active during the out-of-monsoon season, greatly impacts the chemical composition of PM_{10} and PM_1 in the high Himalayas and provides an efficient mechanism for bringing anthropogenic aerosols into the Asian upper troposphere (>5000 m a.s.l.). The concentrations of mineral dust are impacted to a smaller extent by valley breezes and follow a unique seasonal cycle which suggest multiple source areas in central and south-west Asia. Our findings, based on two years of observations of the aerosol chemical composition, provide clear evidence that the southern side of the high Himalayas is impacted by transport of anthropogenic aerosols which constitute the Asian brown cloud.



Correspondence to: S. Decesari
(s.decesari@isac.cnr.it)

1 Introduction

Aerosol measurements performed in south and east Asia over the past decade have shown that the concentration levels of atmospheric particulate matter (PM_{10}) can be of the order of several tenths to some hundreds of µg/m^3 over vast regions, with associated high levels of light-absorbing components (iron oxides and black carbon, BC) (Ramanathan et al., 2001; Verma et al., 2007). Such dense aerosol hazes significantly impact atmospheric transparency and the heating rate of the lower troposphere (Ramanathan et al., 2007a; Dey and Tripathi, 2008). Increasing pollutant emissions associated with the fast-growing economies of south-east Asian countries have led to the progressive increase of aerosol concentrations above the natural background, with a clearly measurable positive trend in the last thirty years (Gautam et al.,

2009a). Satellite observations have shown that the light-absorbing aerosol hazes, or "brown clouds", over India intensify over the Thar desert and the polluted Indo-Gangetic plain, with a sharp boundary to north, where the Himalayas act as a barrier, while extending thousands of miles southward and over the north Indian ocean (e.g., Ramanathan et al., 2007b, Gautam et al., 2009b). These studies suggest that the high Himalayas reside in an area substantially unaffected by the Indian brown clouds and by the dust layers originating from Central Asia (Liu et al., 2008). However, the actual vertical extent of the Indian brown cloud has been measured accurately only since April 2006 by the Cloud Aerosol Lidar and Infrared Pathfinder Satellite (CALIPSO), which has highlighted dense hazes over northern India which can be from 3 to 5 km thick (Ramanathan et al., 2007a). Moreover, aerosol-rich boundary layer air can be transported to higher altitudes by valley breezes on the Himalayan slopes (Hindman and Upadhyay 2002; Gautam et al., 2009a). Analogous processes of vertical transport of pollutants on the slopes of steep mountains have already been observed in Europe in the southern Alpine region (Nyeki et al., 2002).

The transport of optically-active aerosol to the higher Himalayas is matter of concern, since most of the glaciers in the region have been retreating since 1850 (Mayewski and Jeschke, 1979) with increasing melting rates, and are in danger of completely disappearing in the next decades (Anthwa et al., 2006). The retreat of the Himalayan glaciers, if continuing unabated during the 21st century, will exacerbate the water stress in northern India, especially during the dry season. Moreover, the dependence of India on the freshwater supply from the Himalayas is expected to rise in the future, because of the increasing water consumption for industrial and agricultural usages boosted by the rapid economic growth.

We reported first experimental evidence of high black carbon concentrations over the southern slope of high-Himalayas (Bonasoni et al., 2008), at the Nepal Climate Observatory-Pyramid (NCO-P), a permanent aerosol monitoring station located in the Khumbu valley at 5079 m a.s.l. beneath Mt. Everest. An analysis of the results of the first two years of operation of the NCO-P, including BC concentrations and aerosol optical and physical properties, are described in other papers of the present issue. The fine and coarse particulate matter concentrations retrieved from the size distributions measured by online OPC (GRIMM 190) show sharp variations associated with turning breeze regimes and with changes in the air masses. For instance, PM_1 levels can be of $\leq 1\,\mu g/m^3$ in dry descending air originating from the Tibetan plateau, and ranging from 1 to $10\,\mu g/m^3$ in moister air transported from Nepal by up-valley breezes (Marinoni et al., 2010). Such strong variations in the aerosol loads indicate that the NCO-P site intercepted air masses coming from both the middle/upper troposphere and the polluted lower troposphere, thus being in a favourable location, right at the northern rim of the Indian brown cloud, for studying the vertical transport of aerosol hazes towards the high Himalayas and into the middle troposphere over the Indian subcontinent.

2 Experimental

2.1 Sampling

A full description of the Nepal Climate Observatory-Pyramid (NCO-P) is provided by Bonasoni et al. (2008). Briefly, the aerosol and gas instrumentation is sheltered on the top of a hill near to the Pyramid International Laboratory, a multidisciplinary high altitude permanent research centre in the high Khumbu Valley operative since 1990. Although most of the measurements are operated by remote control via satellite connection, the aerosol sampling for off-line chemical analysis relies on the in situ assistance of technicians residing at the Pyramid Laboratory, who perform the change of the filters and store them under refrigeration until they are taken to Kathmandu, where they are sent to the CNR laboratories in Bologna. Technical support is provided by the Ev-K2-CNR Committee and Kathmandu University. At least twice per year, an expedition organized by the Ev-K2-CNR Committee reaches the site for extra maintenance, possible changes of the instrument settings and technical upgrades.

PM_{10} samples have been collected since February 2006 using a home made high-volume (Hi-Vol) system running at $30\,m^3\,h^{-1}$ behind a DIGITEL PM_{10} pre-separator DPM10/30/00. Substrates are quartz-fiber filters (PALL, 15 cm Ø) prefired at 800 °C °C for 1 h. The results discussed here are based on the 99 samples collected up to May 2008. Each of the first six explorative samples was collected over 48 h of continuous sampling, while a sampling schedule differentiating between the two valley breeze regimes was adopted after realizing that the aerosol concentrations varied strongly on average during the day, following the variation of valley breeze direction. Daytime samples with a *maximized* impact from upslope breezes were then collected by sampling from 14:00 to 18:00 (local time) for two consecutive days, while night-time samples with a *minimized* impact of the up-slope valley winds were collected by sampling from 22:00 to 06:00 for two contiguous days. In 2006, some samples were collected also in morning hours in a breeze regime which is fairly similar to that of the nocturnal samples. Normally, one daytime sample and one night-time sample could be collected over a 5-days cycle of operation, but the sampling activities experienced several interruptions due to technical problems or unavailability of electrical power in periods of reduced sunlight (all the instrumentation is powered by photovoltaic panels). Especially in the monsoon season (approximately from June to September, Bonasoni et al., 2010), when the sky remains overcast for most of the day, the power supply has often proved to be insufficient for the Hi-Vol operation, as a result of which only 16 samples were collected

in the summer 2006, most of them during an exceptionally dry event in June, while no samples at all were collected in summer 2007. Therefore, our discussion will focus mainly on the other seasons of the year, providing only preliminary results for the monsoon period.

PM_1 samples were collected using a low-volume system. The 1 µm cut-off was provided by a Digitel DPM10/01/01/0 head at a flow rate of $1\,m^3\,h^{-1}$ kept constant by a vacuum pump behind a critical orifice. Substrates were pre-fired 47 mm quartz-fiber-filters (Whatman). We discuss here the results from the 43 samples collected in the first year of measurements, from February 2007 to February 2008. Daytime PM_1 samples were collected from 13:00 to 18:00 (local time) over three contiguous days, while night-time samples were collected from 22:00 to 06:00 over nine consecutive nights. The long sampling time is necessary given the low sampling flow and the low concentrations typically found during the night.

2.2 Analysis of the mineral fraction

The PM_{10} samples were analysed for their mineral elements by atomic absorption spectroscopy (AAS) after acidic digestion. Only the results for the samples collected up to March 2007 are available so far. About a quarter of each filter was extracted in a microwave oven (maximum temperature: 150 °C; maximum pressure: 60 psi) with 10 ml of concentrated nitric acid + 3.34 ml of hydrogen peroxide solution. After extraction, 7 ml of deionized water were added and the extract was centrifuged. Aliquots of the air particulate matter standard NIST1648 deposited on a blank filter were extracted in parallel to estimate the extraction recovery of the method. Fe, Mg, Ca, K and Na were analyzed by flame (F)-AAS, while Al was analyzed using the graphite furnace (GF-AAS) method.

The mineral fraction was calculated using the equation:

$$\text{Mineral fraction} = 1.16 \times (1.9 \times \text{Al} + 2.15 \times \text{Si} + 2.09 \times \text{Fe} + 1.41 \times \text{Ca} + 1.67 \times \text{Mg}) \text{ (Maenhaut et al., 2002)},$$

where the concentrations of Ca and Mg refer only here to their water-insoluble fraction, and the concentration of Si is inferred from that of Al assuming an average ratio Si/Al=2.5, based on previous results from nearby sites (Carrico et al., 2003).

The concentrations of alkaline metals could not be determined in the samples of summer 2006 due to high blank levels in one batch of filters.

2.3 Analysis of TC, OC, EC, WSOC

Carbonaceous species were analyzed following two distinct methodologies.

Total carbon (TC) and water-soluble organic carbon (WSOC) were analyzed in all PM_{10} and PM_1 samples using a Multi N/C 2100 elemental analyser (Analytik Jena, Germany), equipped with a solid furnace module. For WSOC analyses, aliquots of the quartz fibre filters were extracted in ultra-pure milli-Q water by 30 min sonication. Extracts were filtered on PTFE filters (Sartorius, Germany) to remove quartz fibers and analysed using the same instrumental setup described in Rinaldi et al. (2007). The TC analyses were performed by introducing a small aliquot ($1.3\,cm^2$) of sample into the solid furnace module of the instrument. The sample was exposed inside the combustion chamber to a constant temperature of 950 °C in 100% O_2 and the TC was determined as the total evolved CO_2 by a non-dispersive infrared (NDIR) detector. The instrumental detection limit was 0.2 µg of carbon and the accuracy of the TC measurement was better than 5% for 1 µg of carbon.

Organic carbon (OC) and elemental carbon (EC) were analyzed on a large sub-set (78 out of 99) of PM_{10} samples using the Thermo-Optical Transmission (TOT) method on a Sunset Lab analyzer (Birch and Cary, 1996; Aymoz et al., 2007). The newly developed EUSAAR2 temperature program proposed in Cavalli et al. (2009) was employed. It includes temperature from 200 to 650 °C for the analysis of OC in 100 % He, and up from 500 to 700 °C for the analysis of EC in 98 % He+2% O_2. Automatic split time was always used for the distinction between EC and pyrolysed OC. Fractions of 1.5 cm^2 of the filters were analyzed, without any preparation.

The TC (=OC+EC) concentrations determined by the Sunset Lab analyzer show an excellent agreement (r^2=0.96; slope=0.96) with those determined using the Analytik Jena Multi N/C 2100 analyzer. The PM_1 samples were not analyzed by the Sunset instrument and therefore OC and EC concentrations were not available for PM_1.

The concentrations of TC, OC, EC and WSOC were used to provide an estimate for the total carbonaceous fraction and the total organic fraction, calculated according to the following expressions:

$$\text{Carbonaceous matter} = 1.2 \times (\text{OC} - \text{WSOC}) + 2.0 \times \text{WSOC} + \text{EC}.$$

$$\text{Organic matter} = 1.2 \times (\text{OC} - \text{WSOC}) + 2.0 \times \text{WSOC}$$

Mass-to-carbon ratios of 1.2 and 2.0 were used for water-insoluble and water-soluble organic compounds, respectively, based on assumptions on their oxygen content (Zappoli et al., 1999) and on the functional group composition of the most polar fraction of OC extrapolated from past experiments (Decesari et al., 2007).

2.4 Analysis of inorganic ions

The concentration of inorganic ions (NH_4^+, Na^+, K^+, Ca^{2+}, Mg^{2+}, Cl^-, NO_3^-, SO_4^{2-}) was determined by ion chromatography (IC) using a Dionex ICS-2000 system. Anions were

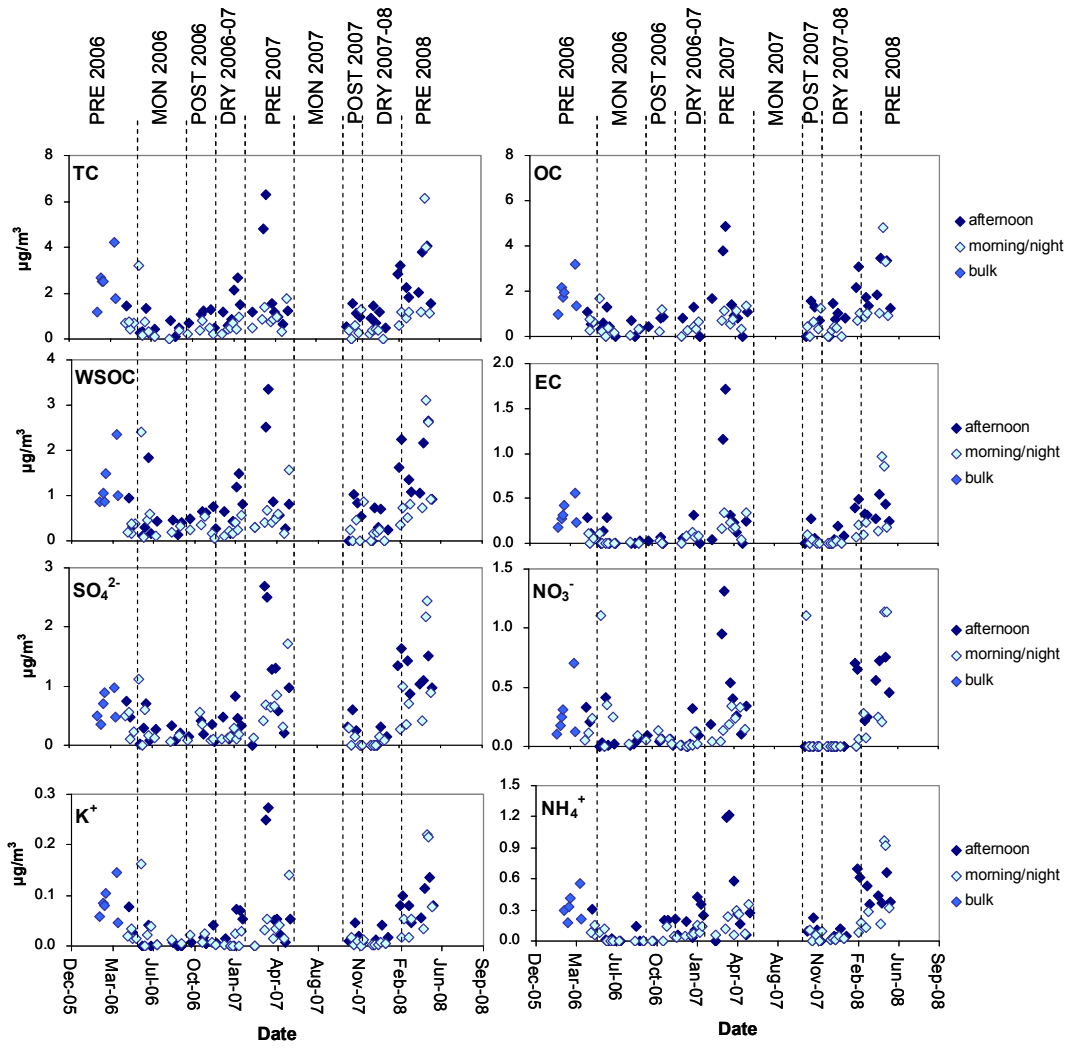


Fig. 1. Concentrations of the main ionic and carbonaceous species in PM_{10} samples.

separated on a IonPac AS11 2×250 mm Dionex separation column with a gradient KOH elution. Cations were separated on a IonPac CS16 3×250 mm Dionex separation column, isocratically with a 30 mM solution of MSA as eluent. Detection limits were of the order of 0.02 and 0.01 µg m^{-3} for each species and for daytime and night-time samplings, respectively.

3 Results

3.1 Seasonality of carbonaceous and ionic species in PM_{10} and PM_1

The time trends of main aerosol chemical components determined on PM_{10} and PM_1 filters are reported in Figs. 1, 2 and 3 and a summary of the aerosol composition observed in the different phases of the yearly monsoon cycle is provided in Tables 1 and 2. The major constituents are organic matter, inorganic salts containing sulphate, ammonium, potassium and calcium with only trace amounts of seasalt, and, in the case of PM_{10}, mineral oxides. The average composition of PM_{10} mass accounted for by carbonaceous and ionic species (Fig. 4) essentially presents the same picture as that found by Carrico and coauthors (2003) in Langtang, at 3920 m a.s.l., approximately 100 km west of NCO-P, showing exactly the same contribution of EC, a very similar contribution from organic compounds and only slightly less sulphate. Seasonally-averaged EC/OC ratios span from 0.11 to 0.18 (Table 3a). Given the limited number of samples, the variations of such ratio between seasons or between day and night samples are not statistically significant. The very small EC content of nocturnal aerosol in the monsoon season is based on only two analyzed samples and therefore must be considered with caution. The average WSOC/OC ratio in PM_{10} varies between 0.6 and 0.8, with the exception of the monsoon season,

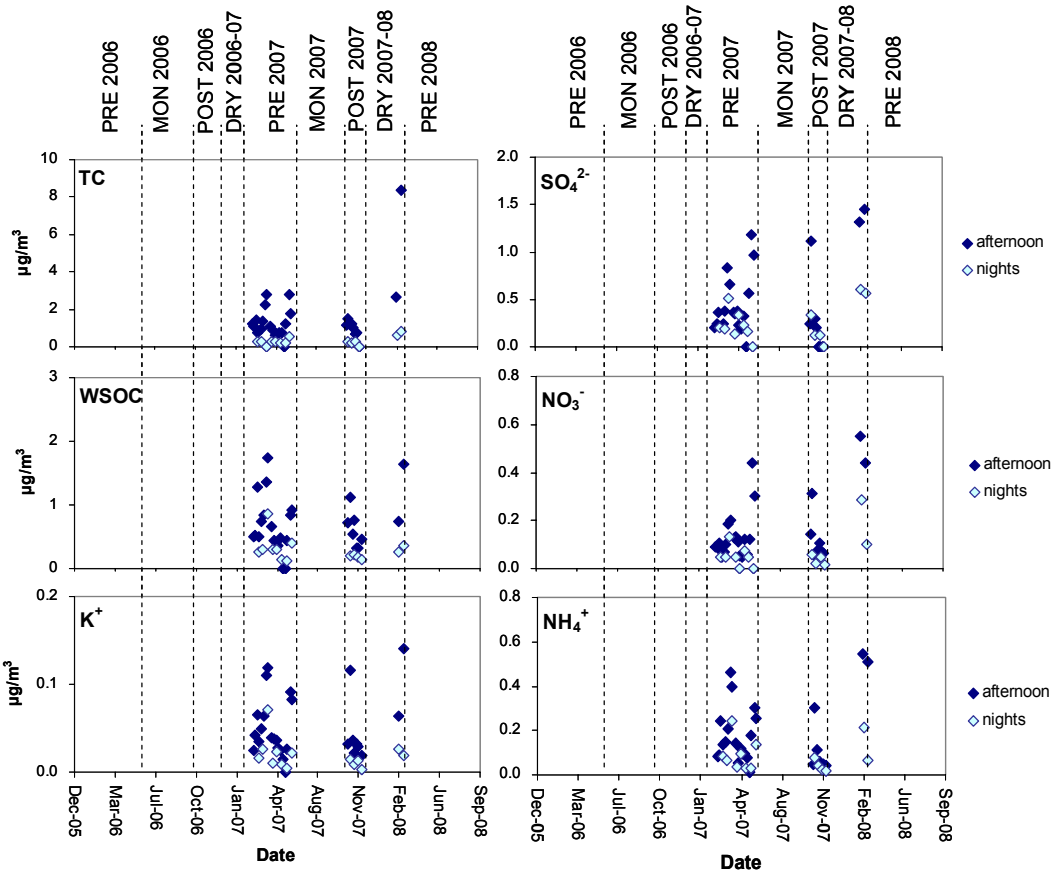


Fig. 2. Concentrations of the main ionic and carbonaceous species in PM_1 samples.

during which aerosol is enriched in water-soluble organic compounds at night-time (Table 3a). High WSOC/OC ratios (>0.6) have already been observed for photochemical haze in suburban and rural environments (e.g., Kumagai et al. 2009), as well as for biomass burning aerosols (e.g., Decesari et al., 2006). A biomass burning source for OC at NCO-P is supported by the good correlation (r^2=0.80) with potassium. However, a more specific discussion of the nature of organic carbon and nitrogen in the NCO-P samples will be presented in a future publication.

At NCO-P, the concentrations of the main chemical species in PM_{10}, including potassium, nitrate, sulphate, ammonium, TC, OC, EC and WSOC, are always higher in daytime than at night-time in all seasons, except for the monsoon period (Table 1). During this season upslope valley winds were observed at the NCO-P also during the night due to the influence of the large-scale summer monsoon circulation (Bonasoni et al., 2010). In the dry season, the difference between daytime and night-time samples is the largest and the concentrations in the valley winds are double than those in the mountain breeze for all species. The PM_1 samples, representative mostly of the premonsoon and postmonsoon periods in 2007, exhibit an analogous behaviour to that of PM_{10} samples, but with a larger excess daytime concentration of TC (Table 2). These results indicate that the diurnal cycle in the aerosol concentrations in the Khumbu Valley, clearly shown by the online PM_{10} and PM_1 measurements using the OPC (Marinoni et al., 2010), is due to the transport of polluted boundary layer air rich in carbonaceous material and ionic chemical species: sulphate and nitrate salts. However, the effect of breeze circulation on concentrations is stronger for potassium and for the carbonaceous species with respect to ammonium nitrate and sulphate salts (Table 1), indicating that the latter are enriched in the background aerosol.

The seasonality of the concentrations of the aerosol chemical components is clearly traced by the time trends of the species determined in PM_{10} samples (Fig. 1, Table 1). The TC, OC, EC and WSOC and the main ionic species share a clear seasonality, which corresponds to the yearly cycle of PM_{10} concentrations described in details in the parallel paper by Marinoni et al. (2010): a peak in the premonsoon period is followed by a minimum in the monsoon season and by a period corresponding to the postmonsoon and dry seasons when the concentrations are also low but still higher than during the monsoon, and that has already been identified as a "ramp-up" period by Carrico et al. (2003) in the time trends

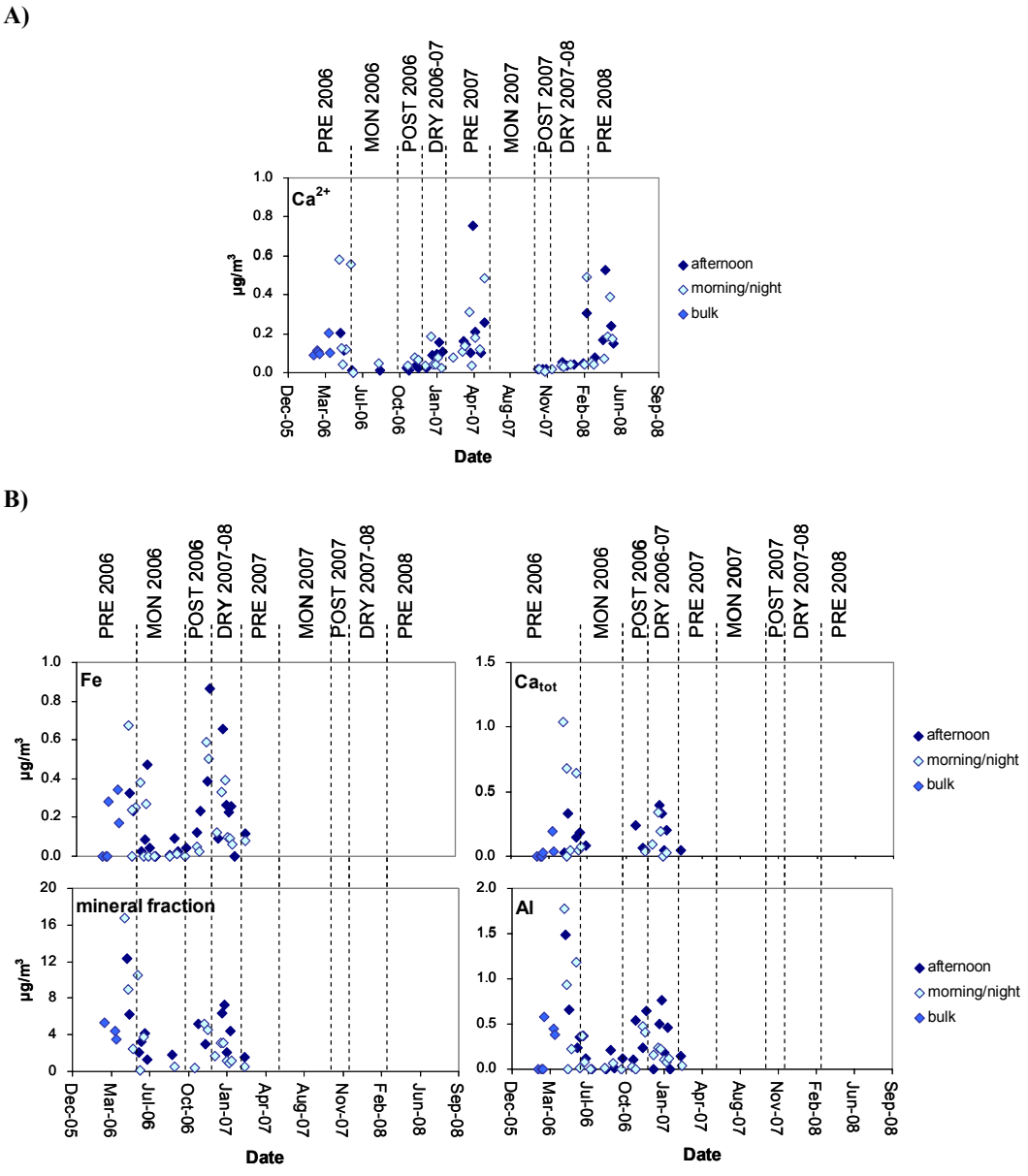


Fig. 3. Concentrations of **(a)** water-soluble calcium and of **(b)** mineral elements in PM_{10} samples. Ca_{tot} stands for total calcium measured by AAS. The mineral fraction concentrations are calculated on the basis of the equation reported in Sect. 2.2.

of $PM_{2.5}$ in Langtang. The similar aerosol phenomenology between Langtang and the high Khumbu Valley suggests that a common transport pattern is responsible for the seasonality of aerosol concentrations along the entire southern side of the upper Nepalese Himalayas, and extending up to at least the altitude of NCO-P (5079 m a.s.l.). The mesoscale circulation in the region has been successfully modelled using WRF simulations (see Bonasoni et al., 2010), showing that upslope breezes provide an efficient way for warm humid (and polluted) air to be transported from the northern edge of the Ganges Plains up to 6000 m a.s.l. in the central upper Himalayas. Higher concentrations in the premonsoon season with respect to the postmonsoon and dry seasons are observed especially in the daytime (D) samples, showing that the high aerosol loads observed in this period of the year are mainly due to the injection of polluted boundary layer air in the high Himalayan valleys through the breeze circulation. Indeed, the occurrence of a large reservoir of pollutants at the foothills of the Himalayas in the premonsoon season is supported by both in-situ (see Sect. 3.3) and satellite measurements (Bonasoni et al., 2010). Although upslope winds are more persistent in the monsoon season, the enhanced precipitation and possibly the decrease in emissions of combustion aerosols from domestic heating in source regions make the

Table 1. Concentrations ($\mu g/m^3$) of the chemical species determined on PM_{10} samples. Statistics are provided for the different seasons and for afternoon and night-time samples, and refer to all the samples collected between April 2006 and May 2008. The number of daytime and night-time samples analyzed in each period of the year are indicated by "*n*" and "*m*", respectively. Data are reported in the format: average (standard deviation), median. However, for the sets including ≤4 samples, only the range of variation is given: (min–max). Notice that the concentrations were calculated using actual measured sampled air volumes. To obtain the concentrations in standard conditions, the values must be multiplied by a factor of 1.8.

		Premonsoon (*n*=26, *m*=19)	Monsoon (*n*=8, *m*=8)	Postmonsoon (*n*=6, *m*=5)	Dry season (*n*=13, *m*=15)
TC	Afternoon	2.2 (1.4), 1.8	0.48 (0.41), 0.37	1.0 (0.36), 1.1	1.1 (0.64), 0.98
	Night	1.4 (1.4), 0.89	0.74 (1.1), 0.34	0.44 (0.31), 0.38	0.46 (0.32), 0.41
OC	Afternoon	1.8 (1.2), 1.5	0.45 (0.41), 0.38	0.83 (0.56), 0.84	0.86 (0.45), 0.81
	Night	1.2 (1.1), 0.89	0.41 (0.58), 0.23	0.49 (0.45), 0.41	0.36 (0.35), 0.31
EC	Afternoon	0.36 (0.36), 0.28	0.06 (0.10), <0.02	0.07 (0.10), 0.04	0.09 (0.11), 0.05
	Night	0.26 (0.26), 0.17	0.02 (0.04), < 0.02	0.03 (0.04), 0.03	0.03 (0.05), < 0.02
WSOC	Afternoon	1.2 (0.83), 0.97	0.48 (0.56), 0.35	0.73 (0.21), 0.65	0.57 (0.42), 0.54
	Night	0.81 (0.80), 0.51	0.55 (0.77), 0.29	0.32 (0.21), 0.35	0.23 (0.24), 0.17
Cl^-	Afternoon	0.023 (0.022), 0.016	< 0.012	< 0.011	0.001 (0.003), <0.010
	Night	0.025 (0.031), 0.012	0.052 (0.13), <0.005	< 0.005	< 0.051
NO_3-	Afternoon	0.41 (0.31), 0.32	0.080 (0.15), 0.025	(0.041–0.093)	0.088 (0.12), 0.041
	Night	0.35 (0.36), 0.24	0.25 (0.36), 0.12	(0.066–0.066)	0.029 (0.039), 0.015
SO_4^{2-}	Afternoon	0.96 (0.65), 0.93	0.23 (0.24), 0.24	0.32 (0.17), 0.27	0.21 (0.26), 0.14
	Night	0.78 (0.64), 0.64	0.29 (0.38), 0.14	0.27 (0.21), 0.28	0.091 (0.083), 0.094
Na^+	Afternoon	0.015 (0.023), <0.022	< 0.039	< 0.039	< 0.037
	Night	0.027 (0.041), <0.013	(<0.016–0.26)	0.009 (0.019), <0.019	0.002 (0.006), <0.018
NH_4^+	Afternoon	0.40 (0.30), 0.34	(<0.023–0.14)	0.17 (0.058), 0.20	0.13 (0.13), 0.060
	Night	0.25 (0.26), 0.17	(<0.009–0.11)	(0.064–0.14)	0.061 (0.044), 0.050
K^+	Afternoon	0.081 (0.065), 0.067	0.008 (0.018), <0.020	0.013 (0.018), 0.005	0.025 (0.027), 0.011
	Night	0.060 (0.065), 0.033	0.036 (0.057), 0.021	0.011 (0.010), 0.009	0.008 (0.010), 0.003
Mg^{2+}	Afternoon	0.016 (0.012), 0.012	0.007 (0.013), <0.019	0.002 (0.002), 0.001	0.001 (0.002), <0.012
	Night	0.021 (0.035), 0.012	0.10 (0.21), 0.021	0.004 (0.006), 0.001	< 0.006
Ca^{2+}	Afternoon	0.17 (0.16), 0.11	< 0.024	0.010 (0.010), 0.016	0.042 (0.049), 0.035
	Night	0.20 (0.17), 0.12	(<0.009-0.56)	(0.008–0.039)	0.056 (0.046), 0.040
Ca	Afternoon	0.10 (0.12), 0.039	0.052 (0.077), <0.02	(<0.02–0.23)	0.16 (0.16), 0.064
	Night	0.44 (0.51), 0.36	0.096 (0.22), < 0.01	< 0.01	0.086 (0.12), 0.033
Mg	Afternoon	0.075 (0.046), 0.081	0.038 (0.047), 0.015	(<0.010–0.055)	0.081 (0.070), 0.070
	Night	0.16 (0.16), 0.12	0.12 (0.26), 0.031	(0.012–0.016)	0.063 (0.038), 0.061
Fe	Afternoon	0.21 (0.12), 0.23	0.093 (0.16), 0.035	(0.042–0.23)	0.39 (0.27), 0.27
	Night	0.31 (0.26), 0.25	0.083 (0.15), 0.001	(0.021–0.046)	0.27 (0.21), 0.23
Na	Afternoon	0.020 (0.024), 0.013	0.008 (0.022), <0.005	(<0.005–0.015)	0.012 (0.019), 0.001
	Night	0.069 (0.13), 0.006	0.065 (0.16), <0.005	(<0.005–0.032)	0.003 (0.004), 0.002
K	Afternoon	0.21 (0.14), 0.21	0.11 (0.12), 0.074	(0.081–0.13)	0.38 (0.19), 0.37
	Night	0.26 (0.18), 0.23	0.13 (0.19), 0.044	(0.071–0.081)	0.21 (0.16), 0.14
Al	Afternoon	0.53 (0.48), 0.44	0.16 (0.15), 0.16	(0.099–0.53)	0.40 (0.27), 0.46
	Night	0.74 (0.79), 0.58	0.22 (0.41), 0.039	(<0.020–0.029)	0.23 (0.14), 0.19
Dust	Afternoon	5.7 (3.7), 5.1	2.2 (1.4), 2.0	(1.0–5.2)	5.1 (2.2), 5.6
	Night	7.5 (7.8), 5.9	(0.14–13)	0.36	2.7 (1.7), 2.5

southerly air masses reaching NCO-P in the summer quite devoid of aerosol particles.

The concentrations of nocturnal samples show a less pronounced but still visible maximum in the premonsoon season, as can be observed especially for sulphate and nitrate, and to a lesser extent in the trends of the carbonaceous species. This suggests that the valley breezes in the premonsoon period can effectively transport pollutants upward impacting the background concentration of the ionic species and partly of the carbon compounds in the middle troposphere. This can be tentatively explained by the fact that the night-time downslope breezes can partially recycle polluted air transported upward during the day (Nyeki et al., 2002; Sellegri et al., 2010).

Although this general transport mechanism of carbonaceous and major ionic species accounts for the positive

Table 2. Concentrations ($\mu g/m^3$) of the chemical species determined on PM_1 samples. Statistics are provided for the periods April–May 2007 (Premonsoon) and October–November 2007 (Postmonsoon) and differentiating between afternoon and night-time samples. The number of daytime and night-time samples analyzed in each period of the year are indicated by "*n*" and "*m*", respectively. Data are reported in the format: average (standard deviation), median. However, for the sets including ≤4 samples, only the range of variation is given: (min–max). Notice that the concentrations were calculated using actual measured sampled air volumes. To obtain the concentrations in standard conditions, the values must be multiplied by a factor of 1.8.

		Premonsoon 2007 (*n*=19, *m*=9)	Postmonsoon 2007 (*n*=7, *m*=4)
TC	Afternoon	1.3 (0.70), 1.1	1.1 (0.31), 1.1
	Night	0.27 (0.12), 0.26	<0.11–0.27
WSOC	Afternoon	0.63 (0.43), 0.49	0.59 (0.28), 0.52
	Night	0.30 (0.22), 0.29	(0.14–0.20)
Cl^-	Afternoon	0.018 (0.017), 0.014	0.031 (0.030), 0.029
	Night	0.004 (0.005), 0.005	(<0.004–0.011)
NO_3^-	Afternoon	0.13 (0.094), 0.11	0.11 (0.088), 0.072
	Night	0.047 (0.039), 0.044	(0.013–0.055)
SO_4^{2-}	Afternoon	0.39 (0.30), 0.35	0.26 (0.38), 0.20
	Night	0.19 (0.15), 0.18	(<0.030–0.32)
Na^+	Afternoon	< 0.12	< 0.26
	Night	< 0.044	< 0.080
NH_4^+	Afternoon	0.16 (0.12), 0.13	0.090 (0.092), 0.047
	Night	0.077 (0.070), 0.064	(0.016–0.076)
K^+	Afternoon	0.046 (0.032), 0.037	0.040 (0.032), 0.031
	Night	0.019 (0.020), 0.015	(0.003–0.014)
Mg^{2+}	Afternoon	0.004 (0.008), <0.005	0.006 (0.016), <0.007
	Night	0.002 (0.003), <0.002	(<0.002–0.006)
Ca^{2+}	Afternoon	0.036 (0.11), <0.090	0.071 (0.19), <0.13
	Night	0.047 (0.059), <0.029	< 0.041

Table 3a. Mass ratios between chemical compounds in PM_{10}. Averages and standard deviations (in parenthesis) are reported. For the sets including ≤4 samples, only the range of variation is given: (min–max). Weighting factors have been applied to EC/TC and WSOC/OC ratios in the low concentration regime (conc. <5×DL) of EC and WSOC.

		EC/TC	WSOC/OC	TC/SO_4^{2-}	NO_3^-/SO_4^{2-}
Premonsoon	Afternoon	0.16 (0.04)	0.69 (0.13)	2.6 (1.4)	0.42 (0.13)
	Night	0.18 (0.06)	0.69 (0.15)	1.9 (0.8)	0.41 (0.12)
Monsoon	Afternoon	(<0.01–0.21)	0.76 (0.25)	1.8 (0.5)	(0.09–0.59)
	Night	(0.01–0.03)*	0.95 (0.16)	2.0 (0.8)	0.94 (0.58)
Postmonsoon	Afternoon	0.11 (0.06)	0.76 (0.13)	3.8 (1.7)	0.35 (0.27)
	Night	(<0.01–0.24)	(0.46–1.0)	(0.7–4.3)	(0.12–0.18)
Dry season	Afternoon	0.13 (0.05)	0.66 (0.19)	3.8 (1.2)	(0.12–0.39)
	Night	0.15 (0.04)	0.75 (0.11)	3.4 (1.1)	0.19 (0.12)

* For the monsoon period and night-time conditions, only two determinations of EC/TC are available.

correlation of their concentrations at NCO-P, the time trends of the specific components do not overlap fully (Fig. 1, Tables 1). In fact, the various aerosol chemical compounds exhibit different sources, either primary or secondary, and the kinetics of formation of the secondary components differ among species. For instance, the enrichment of nitrate with respect to sulphate in the premonsoon period (Fig. 1, Tables 1, 3a) points to a stronger impact from freshly polluted air masses in this period of the year. Very high nitrate mass fractions have been measured also in PM_{10} samples collected during night-time in the monsoon season (Table 3a), but in this case we cannot exclude the possibility of adsorption artefacts promoted by the high relative humidity. Finally, Table 3a shows that sulphate is depleted with respect to total carbon during the dry season, which can be explained by the slower SO_2 oxidation during winter in contrast with the persistence of primary sources of OC and EC.

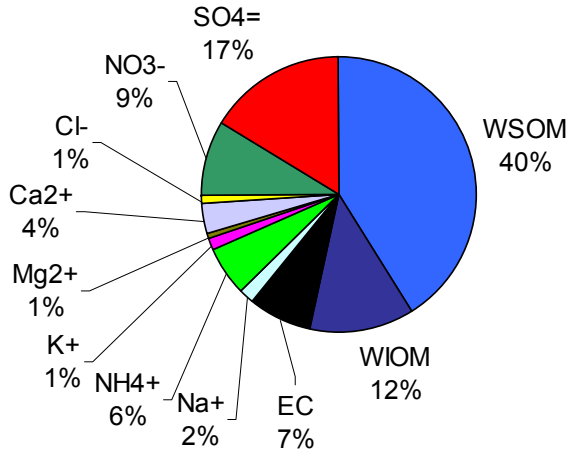


Fig. 4. Average PM_{10} chemical composition with respect to carbonaceous species and major ionic components. Data were derived by the average concentrations of both daytime and afternoon samples in the various seasons weighted for the duration of the samplings and for the average duration of the seasons. Total reconstructed mass amounts to 3.48 µg/m^3 (6.2 µg/scm). WSOM stands for water-soluble organic matter (=WSOC×2), while WIOM is the water-insoluble organic matter ((OC-WSOC)×1.2).

As final remark, we would like to clarify that, even if the valley breeze circulation accounts for the conspicuous increase of the concentrations of most PM_{10} components in daytime in the out-of-monsoon period, peak concentrations of carbonaceous and ionic species are found occasionally also at night (Figs. 1, 2). The OPC data indicate that such periods, e.g., 31 May–2 June 2006, 12–20 June 2006, and 24 April–5 May 2007, 22 May–5 June 2007, 20 April–2 May 2008, were characterized by persistently high PM_1 and PM_{10} concentrations (about 3 times higher than the average over two years of measurements) and by a small difference between day and night, suggesting that the transport of aerosol was forced by synoptic weather systems rather than by the valley winds. The concentration of nitrate was relatively high during these events, indicating that the air masses brought with them fresh pollution. Such observations fit those of Shrestha et al. (2000), who recorded the arrival of high layers of sulphate and nitrate aerosols at Phortse at 4450 m a.s.l. located in a lateral valley to the lower Khumbu Valley, during the premonsoon and monsoon period in 1997. Shrestha and co-authors found that this transport pattern was much more efficient than the valley breeze system in bringing pollutants to the upper Himalayas and could explain why stations at lower altitudes (Jiri at 1900 m a.s.l.) were less polluted, being by-passed by the transport of aerosol layers aloft. By contrast, we found that the transport of polluted air masses associated with the valley breezes overwhelms that caused by episodic synoptic weather patterns throughout the out-of-monsoon season. The discrepancy between our observations and those of Shrestha et al. could be explained by a less favourable location of NCO-P compared to Phortse for being intercepted by the high pollution layers. An alternative explanation is that since the study of Shrestha et al. (2000) in 1997, the distribution and intensity of the aerosol source regions have changed substantially, extending now closer to the Himalayan foothills, thus providing a quasi-continuous supply of aerosol-rich air to the whole southern slope of the central Himalayas through the valley breeze circulation mechanism.

Table 3b. Mass ratios between chemical compounds in PM_1. Averages and standard deviations (in parenthesis) are reported. For the sets including ≤4 samples, only the range of variation is given: (min–max).

		WSOC/TC	TC/SO_4^{2-}	NO_3^-/SO_4^{2-}
Premonsoon	Afternoon	0.58 (0.16)	3.3 (1.1)	0.30 (0.069)
	Night	0.92 (0.20)	1.3 (0.44)	0.29 (0.042)
Postmonsoon	Afternoon	0.57 (0.15)	1.4–4.8	0.16–0.59
	Night	(0.64–1.0)	(0.82–2.3)	(0.16–0.40)

3.2 Mineral fraction

The time trends of the concentrations of mineral elements determined by ion chromatography and AAS in PM_{10} are reported in Fig. 3a, b. The concentrations of iron and calcium in the premonsoon period approximately match those already reported by Giavieri et al. (2005) for the Pyramid Observatory. There is a strong seasonality with peak concentrations between the dry and premonsoon seasons, in agreement with the results from Duchi et al. (2010) who analyzed the frequency of dust transport episodes based on the continuous PM_{10} measurements at NCO-P using the OPC. The concentration of the total mineral fraction can be higher than 5 µg/m^3 in the dry season and as high as 17 µg/m^3 in the premonsoon season (Figure 3b). The analysis of the chemical composition of PM_{10} showed that the maximum in the dry season is more evident for iron, while calcium exhibits a more pronounced maximum during the premonsoon period. Average Fe/Al ratios are 1.1 for the dry season and 0.7 for the premonsoon, while the average Ca/Al ratio is only slightly lower in the dry season (0.6) than in the premonsoon (0.7). The high iron content in the dry period finds confirmation in previous measurements in the Khumbu valley which showed that the Fe/Ca ratio in the postmonsoon is almost double that of the premonsoon period (M. Gallorini, personal communication). Carrico et al. (2003) also reported high Fe/Al ratios (0.5÷0.8) in Langtang, with significant year-to-year variations suggesting different sources for iron and calcium. By analyzing high-resolution ice core data from the northern slope of Mount Everest, Kaspari et al. (2009) concluded that dust deposition in the region is governed by two chemically-distinct populations of mineral aerosols, a first of iron-rich

particles and a second one enriched in calcium, having different origin and providing different contributions with time. Our data indicate that the air concentrations of iron-rich and the calcium-rich mineral aerosols in the Khumbu valley also show a shift in their seasonal cycle.

The seasonality of calcium-rich particles points to common source regions with the anthropogenic aerosol components (see previous section). However, the concentrations of mineral elements and ions in daytime samples are not significantly higher than those in the nocturnal samples with the exception of the dry season (Table 1), indicating that for most of the year mineral particles are not supplied to the site by upslope valley breezes. In other words, the increase of the mineral component of PM_{10} in the premonsoon season is mainly due to an increase in the background concentration and must be related to changes in long-range transport of desert dust particles. By comparing the aerosol composition at 800 m a.s.l. and at 3920 m a.s.l., Carrico et al. (2003) found similar concentrations of Ca at the two stations, in contrast with the carbonaceous species and sulphate aerosols which instead showed a steep gradient. They attributed the homogenous background of mineral particles to long range transport of dust from desert regions in SW Asia and north Africa on the basis of a back-trajectory analysis. On the other hand, a more detailed analysis of the back-trajectories for NCO-P (Bonasoni et al., 2010) shows that long-rang transport from western distal regions is more frequently observed in the dry season than in the premonsoon. In the premonsoon period, a significant fraction of the back-trajectories originates from the Middle-East and in the western Indian subcontinent, including the Thar desert. An analogous source attribution has been proposed for dust storms in the Indo-Gangetic plain (Prasad and Singh, 2007). Satellite data indicate that from the Indo-Gangetic plain the dust-rich aerosols can "climb" the southern slope of the central Himalayas in the premonsoon season (Gautam et al., 2009a). Therefore, a main source region of the calcium-rich particles observed at NCO-P in premonsoon months can be assigned to the arid regions of western India and possibly to upwind regions, like the Arabian deserts. This is also consistent with the results of the chemical analysis, since the composition of TSP or coarse aerosols collected near the Thar desert or in the Arabian sea is characterized by a low iron and a high calcium content: e.g., Ca/Al=1.0, Fe/Al=0.6 (Rastogi and Sarin, 2009); Ca/Al=0.9, Fe/Al=0.5 (Kumar et al., 2008).

In respect to the origin of iron-rich particles in winter, it must be kept in mind that although dust emissions in Asia peak in spring (Shao and Dong, 2006), the transport of dust to the southern Tibetan and Himalayan region is more efficient in winter because of the shift of the 500 hPa jet stream toward south during the dry season (Han et al., 2008). Kaspari et al. (2009) found a correlation between the deposition of iron-rich dust particles on the northeast ridge of Mount Everest with the emission from distal sources in Africa and in the middle East. According to that study, the frequency of African and Arabian desert dust deposition in the Himalayas is maximum in January. Although the back-trajectories calculated for NCO-P support a prevalent transport pattern from west during the dry season, such long-range transport occurs mainly in the upper troposphere (>4000 m above the ground), with no clear evidence of lifting air masses from dust source regions in Africa and in the middle East (Bonasoni et al., 2010; Duchi et al., 2010). Therefore, the origin of iron-rich dust particles in the dry season cannot be clarified at the moment. The analysis of a longer series of PM_{10} samples by AAS together with the study of the back-trajectories for specific events will allow a better identification of the transport mechanisms and source regions of dust particles in the Khumbu Valley.

3.3 Comparison with other measurements in Tibet and in the Indian subcontinent

Table 4a reports the seasonally-averaged concentrations of carbonaceous and ionic species at the NCO-P site, in comparison to the concentrations measured at neighbouring mountain stations in past studies. A second Table 4b shows the results of the measurements performed at other sites in the Indian subcontinent, where major source areas for the aerosol transported to NCO-P are located. The comparison of mineral dust aerosol concentrations between NCO-P and the other Nepalese, Chinese and Indian stations cannot be discussed here because of the sparse literature data available and due to the different metrics used (water-soluble calcium, total calcium, mineral elements, "total dust") and different sampling cut-offs adopted in the various studies.

The concentrations of carbonaceous aerosols in the Himalayas decrease steeply with altitude in out-of-monsoon periods and the concentration levels in Nagarkot (2150 m a.s.l.) are 5–6 times higher than at NCO-P. On the other hand, during the monsoon season the difference is not significant, although we acknowledge that the average values for NCO-P are based on a small set of samples in this period of the year, and are probably biased towards relatively more polluted conditions. The concentrations in urban sites located within high-altitude basins, as in Lhasa, can be one order of magnitude higher than those found in the present study. The concentrations at mountain sites in western India, despite of their lower altitudes, are not significantly higher than in Nagarkot, suggesting that the Nepalese sector of the Himalayas is relatively more polluted, which is in agreement with the satellite measurements presented by Gautam et al., 2009a. Interestingly, the difference in TC (or OC) concentrations among the mountain sites (Table 4a) and the very polluted urban sites in the Indian subcontinent (Table 4b) tends to magnify in winter. During the premonsoon period, the concentrations in the megacities are about only twice those at the Himalayan foothills (Nagarkot) and about one order of magnitude higher than those at NCO-P, while during the post-monsoon/dry periods the difference in concentration between

Table 4a. Concentrations of main aerosol chemical species at NCO-P compared to other mountain stations in Nepal, China and India. Data are provided in μg scm^{-1} (standard cubic meters). [a] This study; [b] Shrestha et al., 2000; [c] Carrico et al., 2003; [d] Ming et al., 2007; [e] Zhang et al., 2008; [f] Rengarajan et al., 2007; [g] Ram et al., 2008; [h] Rastogi and Sarin, 2005.

Site name	Altitude (m a.s.l.)	Sample type	Season	TC	OC	EC	SO_4^{2-}	NO_3^-	NH_4^+	K^+	Ca^{2+}
NCO-P, Nepal[a]	5079	PM_{10}	premonsoon	2.8	2.4	0.5	1.48	0.66	0.52	0.12	0.34
			monsoon	1.2	0.9	0.1	0.50	0.37	0.00	0.05	0.00
			postmonsoon	1.2	1.4	0.1	0.50	0.00	0.08	0.02	0.01
			dry season	1.3	1.2	0.1	0.22	0.08	0.14	0.02	0.10
Phortse, Nepal[b]	4450	PM_8	premonsoon				0.94	1.5	1.6	0.50	0.19
			monsoon				0.17	0.34	0.26	0.15	0.03
			postmonsoon				0.10	0.09	0.19	0.05	0.02
			dry season				0.18	0.23	0.15	0.07	0.05
Langtang, Nepal[c]	3920	$PM_{2.5}$	premonsoon		3.4	0.5	1.4	0.78	0.54	0.20	0.66
			monsoon		0.8	0.2	0.20	0.09	0.08	0.01	0.10
			postmonsoon/dry season		1.8	0.5	0.27	0.04	0.15	0.02	0.03
Nagarkot, Nepal[c]	2150	$PM_{2.5}$	premonsoon		14	1.5	3.8	1.2	1.5	0.62	0.31
			monsoon		2.0	0.5	0.80	0.08	0.25	0.04	0.07
			postmonsoon/dry season		6.3	1.0	2.5	0.80	1.20	0.28	0.05
Jiri, Nepal[b]	1900	PM_8	premonsoon				0.48	0.46	0.38	0.26	0.28
			monsoon				0.12	0.02	0.14	0.08	0.02
			postmonsoon				0.20	0.06	0.20	0.10	0.04
			dry season				0.48	0.86	0.62	0.21	0.11
Rongbuk Glacier, China[d]	6500	TSP	monsoon				0.41	0.14		0.02	0.04
Lhasa, China[e]	3363	PM_{10}	premonsoon		35	6					
			monsoon		19	2.5					
			postmonsoon		17	3					
			dry season		18	4					
Manora Peak, India[f,g]	1950	TSP	dry season	5.8			2.6	0.5	0.52	0.23	0.75
			dry season/premonsoon		∼10	1.5					
			monsoon		2–6	0.3–0.4					
			postmonsoon		6–10	0.9–1.3					
Mt. Abu, west India[g,h]	1680	TSP	dry season/premonsoon		3.5	0.1–0.8					
			monsoon		2.2	0.1	2.7	0.43		0.13	2.4
			postmonsoon		4.9	0.7					
			out of monsoon				2.6	0.74	0.37	0.2	1.7

Table 4b. Summary of literature data on main aerosol chemical species concentrations in the Indian subcontinent. [a] Rengarajan et al., 2007; [b] Rastogi and Sarin, 2005 (inorganic ion data); [c] Rastogi and Sarin 2009 (OC and EC data); [d] Chowdhury et al., 2007 (OC and EC data); [e] Venkataraman et al., 2002 (inorganic ions data, only for Mumbai); [f] Nair et al., 2006; [g] George et al., 2008; [h] Salam et al., 2003; [i] Mayol-Bracero et al. 2002; [j] Sudheer and Sarin, 2008.

Site name	Sample type	Season	TC	OC	EC	SO_4^{2-}	NO_3^-	NH_4^+	K^+	Ca^{2+}
Hisar (urban, north-west India)[a]	TSP	dry season	37			13	13	6.3	2.4	3.5
Ahmedabad (urban, west India)[b,c]	TSP	premonsoon		13	2.1					
		monsoon		6.6	0.7	3.1	0.94	0.05	0.2	2.5
		postmonsoon		16	3.3					
		dry season		19	3					
		postmonsoon/dry season/premonsoon				4.5	2.1	0.48	0.76	3.0
Delhi, Mumbai, Kolkata (megacities, India)[d,e]	$PM_{2.5}$	premonsoon		10 – 38	4 - 9					
		monsoon		8–16	4–7					
		postmonsoon		18–57	6–12					
		dry season		34–147	12–27	6.8	4.7		13	3.2
		premonsoon				4.9	1.6	1.2	0.5	
urban and rural sites in south India [f,g]	TSP, PM_{10}	monsoon				3.9	1.8	0.2	0.6	
		postmonsoon/dry season				3–10	1–4	1–2	0.4–1	0.6–4
Dhaka (megacity, Bangladesh)[h]	TSP	dry season	68	46	22	11	3.6	1.9	1.6	6.8
INDOEX campaign (north Indian Ocean)[i]	$PM_{1.3}$	dry season/premonsoon	5.7	3.4	2.5	5.6	0.16	1.8	0.34	
Bay of Bengal[j]	TSP	premonsoon		0.3–5.5	0.1–0.7					
		dry season		2–8	0.4–3.4					

the megacities and the mountain sites ranges between one order of magnitude (Nagarkot) and almost two orders of magnitude (NCO-P). This confirms that during the postmonsoon and the dry season, a significant fraction of pollution aerosols is trapped at the lower altitudes, while during the premonsoon period the concentrations increase at all sites and the vertical gradient reaches a minimum.

The comparison of the inorganic ionic components concentrations shows a slightly different picture. Sulphate concentrations can be higher than 10 $\mu g/m^3$ in the dry period at urban sites, but it spans between 3 and 6 $\mu g/m^3$ at most locations, including the Indian Ocean in the dry and premonsoon seasons (Mayol-Bracero et al., 2002) (Table 4b). Compared to this regional background, the mountain sites in western and northern India and in the lower Himalayas are only slightly depleted in sulphate aerosol ($\sim$2–4 $\mu g/m^3$), while the stations in the higher Himalayas show a common pattern with concentrations of about 1 $\mu g/m^3$ in the premonsoon season and $0.5 \leq \mu g/m^3$ in the other periods (Table 4a). Therefore, the concentrations in the high Himalayas are only five- to tenfold lower than those measured of the polluted areas in the Indian subcontinent, indicating that sulphate aerosols are more spatially homogeneously distributed compared to carbonaceous aerosols, which is consistent with the different sources for these two aerosol components: essentially secondary for the former and mixed primary and secondary for the latter. This implicates that the potential source region for the sulphate aerosols observed at NCO-P is wider than for the carbonaceous particles, for which a greater impact from proximal (primary) sources must be expected. Based on this evidence and on the dependence of carbonaceous particle concentrations on breeze regimes (see Sect. 3.1), we hypothesize that the OC and EC concentration levels at NCO-P depends more on Nepalese primary sources than on emissions distributed over the whole Indian subcontinent. The rapid upward transport of primary carbonaceous particles through orographic venting is responsible for the significantly higher TC/SO_4^{2-} ratios observed in the region (Table 3a, b) compared to the remote areas at the southern fringes of the Asian brown cloud (Table 4b, Mayol-Bracero et al., 2002).

4 Conclusions

The chemical composition of PM_{10} and PM_1 and the time trends of the chemical constituents observed at the Nepal Climate Observatory-Pyramid in the period April 2006–May 2008 exhibit striking similarities with the results provided by the only previous study reporting complete chemical composition data for a high-altitude Nepalese station (Carrico et al., 2003).

As in Langtang, the carbonaceous species are very abundant (TC=1$\div$4 $\mu g\,scm^{-1}$ as seasonal averages) and their concentrations predominate over those of total inorganic ions, on average.

We provide new results on the chemical composition of aerosol in Himalayan valleys collected under different breeze regimes. Our data indicate that the systematic increase in the concentrations of PM_1 and PM_{10} associated with the upslope breezes blowing in afternoon hours must be attributed especially to the transport of carbonaceous aerosols, and to a lesser extent to nitrate and sulphate aerosols, and, in the dry season, also to mineral dust.

Overall, our observations support the previous sparse in situ measurements and the remote sensing data indicating that the southern side of the higher Himalayas are impacted by the upward transport of pollutants from a large reservoir in the lower Nepalese provinces and/or upwind regions, which represents the northern rim of the Indian brown cloud.

It was found that sulphate concentrations at NCO-P are comparable to those previously observed at other high-altitude Himalayan stations and five- to tenfold lower than in the polluted areas of the Indian subcontinent. The vertical gradient of carbonaceous aerosol concentration is generally steeper, especially in the dry season, with differences of up to two orders of magnitude between NCO-P the most polluted urban areas in India. Contrary to the sulphate concentration which exhibits a relatively high background at NCO-P, the carbonaceous aerosol concentration is controlled prevalently by the direct upward injection of boundary layer air through the valley-breeze circulation.

Mineral dust is the main component of PM_{10} at NCO-P and its seasonally-averaged concentrations span between 0.5 and 10 $\mu g\,scm^{-1}$. The time trend of the concentrations of calcium-rich particles indicate that they are transported to NCO-P from the south mixed with pollution aerosols and must originate in the Indian subcontinent or in upwind regions through a long-range transport. Evidence was found of additional mineral dust sources, active especially in the dry season, and which could not be fully explained for the time being, but which may indicate an impact of dust emissions in central Asia or of long-range transport from far off western arid regions.

Acknowledgements. This work was carried out in the framework of the UNEP – ABC (Atmospheric Brown Clouds) and EvK2CNR – SHARE (Stations at High Altitude for Research on the Environment) projects. We thank Tenzing Chhottar Sherpa, Kaji Bista, Laxman Adhikary, Pema Sherpa, Lhakpa Tshering Sherpa, Lakpa Tenzi Sherpa, Chhimi Tenzing Sherpa and Hari Shrestha for their support at the Nepal Climate Observatory -Pyramid.

Edited by: G. McFiggans

References

Ashish, A., Joshi, V., Sharma, A., and Anthwal, S.: Retreat of Himalayan glaciers indicator of climate change, Nature and Science, 4(4), 53–60, 2006.

Aymoz, G., Jaffrezo, J. L., Chapuis, D., Cozic, J., and Maenhaut, W.: Seasonal variation of PM_{10} main constituents in two valleys

of the French Alps. I: EC/OC fractions, Atmos. Chem. Phys., 7, 661–675, doi:10.5194/acp-7-661-2007, 2007.

Birch, M. E. and Cary, R. A.: Elemental carbon-based method for monitoring occupational exposures to particulate diesel exhaust, Aerosol Sci. Tech., 25, 221–241, 1996.

Bonasoni, P., Laj, P., F. Angelini, Arduini, J., Bonafè, U., Calzolari, F. P., Cristofanelli, P., Decesari, S., Facchini, M. C., Fuzzi, S., Gobbi, G.P., Maione, M., Marinoni, A., Petzold, A., Roccato, F., Roger, J. C., Sellegri, K., Sprenger, M., Venzac, H., Verza, G.P., Villani, P., and Vuillermoz, E.: The ABC-Pyramid Atmospheric Research Observatory in Himalaya for aerosol, ozone and halocarbon measurements, Sci. Tot. Environ., 391, 252–261, 2008.

Carrico, C. M., Bergin, M. H., Shrestha, A. B., Dibb, J. E., Gomes, L., and Harris, J. M., The importance of carbon and mineral dust to seasonal aerosol properties in the Nepal Himalaya, Atmos. Environ., 37, 20, 2811–2824, 2003.

Cristofanelli, P., Bracci, A., Sprenger, M., Marinoni, A., Bonaf, U., Calzolari, F., Duchi, R., Laj, P., Pichon, J. M., Roccato, F., Venzac, H., Vuillermoz, E., and Bonasoni, P.: Tropospheric ozone variations at the Nepal climate observatory pyramid (Himalayas, 5079 m a.s.l.) and influence of stratospheric intrusion events, Atmos. Chem. Phys. Discuss., 10, 1483–1516, doi:10.5194/acpd-10-1483-2010, 2010.

Chowdhury, Z., M., Zheng, J. J., Schauer, R. J., Sheesley, L. G., Salmon, G. R., Cass, and Russell, A. G.: Speciation of ambient fine organic carbon particles and source apportionment of $PM_{2.5}$ in Indian cities, J. Geophys. Res., 112, D15303, doi:10.1029/2007JD008386, 2007.

Decesari, S., Fuzzi, S., Facchini, M. C., Mircea, M., Emblico, L., Cavalli, F., Maenhaut, W., Chi, X., Schkolnik, G., Falkovich, A., Rudich, Y., Claeys, M., Pashynska, V., Vas, G., Kourtchev, I., Vermeylen, R., Hoffer, A., Andreae, M. O., Tagliavini, E., Moretti, F., and Artaxo, P.: Characterization of the organic composition of aerosols from Rondnia, Brazil, during the LBA-SMOCC 2002 experiment and its representation through model compounds, Atmos. Chem. Phys., 6, 375–402, doi:10.5194/acp-6-375-2006, 2006.

Dey, S. and Tripathi, S. N.: Aerosol direct radiative effects over Kanpur in the Indo-Gangetic basin, northern India: Long-term (2001–2005) observations and implications to regional climate, J. Geophys. Res., 113, D04212, doi:10.1029/2007JD009029, 2008.

Duchi, R., Cristofanelli, P., Marinoni, A., Angelici, F., et al.: Continuous dust synoptic transport observations at the Nepal Climate Observatory-Pyramid (5079 m a.s.l.) in the Himalayas, Atmos. Chem. Phys. Discuss. in preparation, 2010.

Gautam, R., Hsu, N. C., Lau, K. M., Tsay, S. C., and Kafatos, M.: Enhanced pre-monsoon warming over the Himalayan-Gangetic region from 1979 to 2007, Geophys. Res. Lett., 36, L07704, doi:10.1029/2009GL037641, 2009a.

Gautam, R., Liu, Z., Singh, R. P., and Hsu, N. C.: Two constrasting dust-dominant periods over India observed from MODIS and CALIPSO, Goephys. Res. Lett., 36, L06813, doi:10.1029/2008GL036967, 2009b.

George, S. K., Nair, P. R., Parameswaran, K., Jacob, S., and Abraham, A.: Seasonal trends in chemical composition of aerosols at a tropical coastal site of India, J. Geophys. Res., 113, D16209, doi:10.1029/2007JD009507, 2008.

Giaveri, G., Bergamaschi, L., Rizzio, E., Verza, G., Zambelli, G., Brandone, A., Profumo, A., Baudo, R., Tartari, G., and Gallorini, M.: INAA at the top of the world: Elemental characterization and analysis of airborne particulate matter collected in the Himalayas at 5100 m high, J. Radioanal. Nucl. Ch., 263, 725–732, 2005.

Han, Y., Fang, X., Kang, S., Wang, H., and Kang, F.: Shifts of dust source regions over central Asia and the Tibetan Plateau: Connections with the Arctic oscillation and the westerly jet, Atmos. Environ., 42, 10, 2358–2368, 2008.

Hindman, E. E. and Upadhyay, B. P.: Air pollution transport in the Himalayas of Nepal and Tibet during the 1995–1996 dry season, Atmos. Environ., 36, 727–739, 2002.

Kaspari, S., Mayewski, P. A., Handley, M., Kang, S., Hou, S., Sneed, S., Maasch, K., and Qin, D.: A high-resolution record of atmospheric dust composition and variability since A.D. 1650 from a Mount Everest ice core, J. Climate, 22, 3910–3925, 2009.

Kumagai, K., Iijima, A., Tago, H., Tomioka, A., Kozawa, K., and Sakamoto, K.: Seasonal characteristics of water-soluble organic carbon in atmospheric particles in the inland Kanto plain, Japan. Atmos. Environ., 43, 3345–3351, 2009.

Liu, Z., Liu, D., Huang, J., Vaughan, M., Uno, I., Sugimoto, N., Kittaka, C., Trepte, C., Wang, Z., Hostetler, C., and Winker, D.: Airborne dust distributions over the Tibetan Plateau and surrounding areas derived from the first year of CALIPSO lidar observations, Atmos. Chem. Phys., 8, 5045–5060, doi:10.5194/acp-8-5045-2008, 2008.

Maenhaut, W., Schwarz, J., Cafmeyer, J., and Chi, X.: Aerosol chemical mass closure during the EUROTRAC-2 AEROSOL Intercomparison 2000, Nucl. Instr. Meth. Phys. Res., Sec. B, 189, 233–237, 2002.

Marinoni, A., Cristofanelli, P., Laj, P. et al.: Aerosol mass and black carbon concentrations, two year-round observations at NCO-P (5079 m, southern Himalayas), Atmos Chem. Phys. Discuss., in preparation, 2010.

Mayol-Bracero, O. L., Gabriel, R., Andreae, M. O., Kirchstetter, T. W., Novakov, T., Ogren, J., Sheridan, P., and Streets, D. G.: Carbonaceous aerosols over the Indian Ocean during the Indian Ocean Experiment (INDOEX): Chemical characterization, optical properties, and probable sources, J. Geophys. Res., 107, D198030, doi:10.1029/2000JD000039, 2002.

Ming, J., Zhang, D., Kang, S., and Tian, W.: Aerosol and fresh snow chemistry in the East Rongbuk Glacier on the northern slope of Mt. Qomolangma (Everest), J. Geophys. Res., 112, D15307, doi:10.1029/2007JD008618, 2007.

Nair, P. R., George, S. K., Sunilkumar, S. V., Parameswaran, K., Jacub, S., and Abraham, A.: Chemical composition of aerosols over peninsular India during winter, Atmos. Environ., 40, 6477–6493, 2006.

Nyeki, S., Eleftheriadis, K., Baltensperger, U., Colbeck, I., Fiebig, M., Fix, A., Kiemle, C., Lazaridis, M., and Petzold, A.: Airborne lidar and in-situ aerosol observations of an elevated layer, leeward of the European Alps and Apennines, Geophys. Res. Lett., 29(17), 1852, doi:10.1029/2002GL014897, 2002.

Owen, L. A. and Sharpa, M. C.: Rates and magnitudes of paraglacial fan formation in the Garhwal Himalaya: implications for landscape evolution, Geomorphology, 26, 171–184, 1998.

Prasad, A. K. and Singh, R. P.: Changes in aerosol parameters during major dust storm events (2001–2005) over the Indo-Gangetic Plains using AERONET and MODIS data, J. Geophys. Res., 112, D09208, doi:10.1029/2006JD007778, 2007.

Ram, K., Sarin, M. M., and Hedge, P.: Atmospheric abundances of primary and secondary carbonaceous species at two high-altitude sites in India: Sources and temporal variability, Atmos. Environ., 42, 6785–6796, 2008.

Ramanathan, V., Crutzen, P. J., Lelieveld, J., et al.: Indian Ocean Experiment: An integrated analysis of the climate forcing and effects of the great Indo-Asian haze, J. Geophys. Res., 106, 28371–28398, 2001.

Ramanathan, V., Ramana, M. V., Roberts, G., Kim, D., Corrigan, C., Chung, C., and Winkler, D.: Warming trends in Asia amplified by brown cloud solar absorption, Nature, 448, 575–578, 2007a.

Ramanathan, V., Li, F., Ramana, M. V., Siva, P. S., Kim, D., Corrigan, C. E., Nguyen, H., Stone, E. A., Schauer, J. J., Carmichael, G. R., Adhikary, B., and Yoon, S. C.: Atmospheric Brown Clouds: Hemispherical and regional variations in long range transport, absorption and radiative forcing, J. Geophys. Res., 112, D22S21, doi:10.1029/2006JD008124, 2007b.

Rastogi, N. and Sarin, M. M.: Long-term characterization of ionic species in aerosols from urban and high-altitude sites in western India: Role of mineral dust and anthropogenic sources, Atmos. Environ., 39, 5541–5554, 2005.

Rastogi, N. and Sarin, M. M.: Quantitative chemical composition and characteristics of aerosols over western India: One-year record of temporal variability, Atmos. Environ., 43, 3481–3488, 2009.

Rengarajan, R., Sarin, M. M., and Sudheer, A. K.: Carbonaceous and inorganic species in atmospheric aerosols during wintertime over urban and high-altitude sites in North India, J. Geophys. Res., 112, D21307, doi:10.1029/2006JD008150, 2007.

Rinaldi, M., Emblico, L., Decesari, S., Fuzzi, S., Facchini, M. C., and Librando, V: Chemical Characterization and Source Apportionment of Size-Segregated Aerosol Collected at an Urban Site in Sicily, Water, Air and Soil Pollution, 185, 311–321, 2007.

Salam, A., Bauer, H., Kassin, K., Ullah, S. M., and Puxbaum, H.: Aerosol chemical characteristics of a mega-city in Southeast Asia (Dhaka–Bangladesh), Atmos. Environ., 37, 2517–2528, 2003.

Sellegri, K., Laj, P., Venzac, H., Boulon, J., Picard, D., Villani, P., Bonasoni, P., Marinoni, A., Cristofanelli, P., and Vuillermoz, E.: Seasonal variations of aerosol size distributions based on long-term measurements at the high altitude Himalayan site of Nepal Climate Observatory-Pyramid (5079 m), Nepal, Atmos. Chem. Phys. Discuss., 10, 6537–6566, doi:10.5194/acpd-10-6537-2010, 2010.

Shao, Y. and Dong, C. H.: A review on East Asian dust storm climate, modelling and monitoring, Global and Planetary Change, 52, 1–22, 2006.

Shrestha, A. B., Wake, C. P., Dibb, J. E., Mayewski, P. A., Whitlow, S. I., Carmichael, G. R., and Ferm, M.: Seasonal variations in aerosol concentrations and compositions in the Nepal Himalaya, Atmos. Environ., 34, 3349–3363, 2000.

Sudheer, A. K. and Sarin, M.M.: Carbonaceous aerosols in MABL of Bay of Bengal: Influence of continental outflow, Atmos. Environ., 42, 4089–4100, 2008.

Venkataraman, C., Reddy, C. K., Josson, S., and Reddy, M. S.: Aerosol size and chemical characteristics at Mumbai, India, during the INDOEX-IFP (1999), Atmos. Environ., 36, 1979–1991, 2002.

Verma, S., Venkataraman, C., Boucher, O., and Ramachandran, S.: Source evaluation of aerosols measured during the Indian Ocean Experiment using combined chemical transport and back trajectory modeling, J. Geophys. Res., 112, D11210, doi:10.1029/2006JD007698, 2007.

Zappoli, S., Andracchio, A., Fuzzi, S., Facchini, M. C. A., Gelencser, A., Kiss, G., Krivacsy, Z., Molnár, A., Meszaros, E., Hansson, H. C., Rosman, K., and Zebuhr, Y.: Inorganic, organic and macromolecular components of fine aerosol in different areas of Europe in relation to their water solubility, Atmos. Environ., 33, 2733–2743, 1999.

Zhang, X. Y., Wang, Y. Q., Zhang, X. C., Guo, W., and Gong, S. L.: Carbonaceous aerosol composition over various regions of China during 2006, J. Geophys. Res., 113, D14111, doi:10.1029/2007JD009525, 2008.